HHS Public Access

Author manuscript

Top Magn Reson Imaging. Author manuscript; available in PMC 2019 October 01.

Published in final edited form as:

Top Magn Reson Imaging. 2018 October ; 27(5): 305–318. doi:10.1097/RMR.0000000000000178.

Stiffness and beyond: what MR elastography can tell us about brain structure and function under physiologic and pathologic conditions

Ziying Yin, Ph.D.[1], **Anthony J. Romano, Ph.D.**[2], **Armando Manduca, Ph.D.**[1,3], **Richard L. Ehman, M.D.**[1], and **John Huston III, M.D.**[1,*]

[1]Department of Radiology, Mayo Clinic College of Medicine, Rochester, MN

[2]Naval Research Laboratory, Washington, DC

[3]Departments of Physiology and Biomedical Engineering, Mayo Clinic College of Medicine, Rochester, MN

Abstract

Brain MR elastography (MRE) was developed based on a desire to “palpate by imaging” and is becoming a powerful tool in the investigation of neurophysiological and neuropathological states. Measurements are acquired with a specialized MR phase-contrast pulse sequence that can detect tissue motion in response to an applied external or internal excitation. The tissue viscoelasticity is then reconstructed from the measured displacement. Quantitative characterization of brain viscoelastic behaviors provides us an insight into the brain structure and function by assessing the mechanical rigidity, viscosity, friction, and connectivity of brain tissues. Changes in these features are associated with inflammation, demyelination, and neurodegeneration that contribute to brain disease onset and progression. Here, we review the basic principles and limitations of brain MRE and summarize its current neuroanatomical studies and clinical applications to the most common neurosurgical and neurodegenerative disorders, including intracranial tumors, dementia, multiple sclerosis, amyotrophic lateral sclerosis, and traumatic brain injury. Going forward, further improvement in acquisition techniques, stable inverse reconstruction algorithms, and advanced numerical, physical, and preclinical validation models are needed to increase the utility of brain MRE in both research and clinical applications.

Keywords

magnetic resonance elastography; brain; stiffness; viscoelasticity; slip interface imaging; intracranial tumors; dementia; neurodegenerative diseases; multiple sclerosis

Since its inception in 1995,[1] MR elastography (MRE), developed on a desire to “palpate by imaging,” has been evolving and becoming a powerful tool in the investigation of tissue physiological and pathological states in various organs including the brain. Studying the brain with MRE is unique because by analyzing the induced brain motion in response to

*Corresponding author: John Huston III, MD, jhuston@mayo.edu, +1 507-284-2511 (O), 200 1st St SW # W4, Rochester, MN 55905, USA.

intrinsic and extrinsic excitation, qualitative and quantitative measures of tissue mechanical properties can be assessed noninvasively, which is not possible with other imaging modalities. The noninvasive characterization of brain mechanical behaviors provides unique clues to the mechanical rigidity, viscosity, friction, and connectivity of tissues and to changes in those features accompanying inflammation, demyelination, and neurodegeneration during the onset and progression of brain diseases.[2,3]

In this review paper, we will provide a brief background to the principles of brain MRE, discuss MRE-derived quantitative and qualitative parameters, summarize its applications to various neurosurgical and neurodegenerative disorders as well as neuroanatomical studies, and highlight current challenges and opportunities for future research.

Principles of Brain MRE and Key Concepts

Brain MRE involves the following three processes: generating shear waves within the intracranial brain tissue by an external driver, imaging the propagation of the induced shear waves using a phase-contrast MR pulse sequence, and processing the shear waves to create elastograms, which are quantitative maps of tissue stiffness. The following provides a brief summary of each step, current techniques, and associated key concepts. More in-depth reviews of elastography physics can be found elsewhere.[4–6]

How brain MRE images are obtained

With brain MRE, the shear waves are most commonly generated by means of an external driver system which vibrates the entire head transmitting motion from the skull into the brain tissue. The external driver system consists of an active driver as the vibration source for generating oscillation and a passive driver that provides contact between the driver and subject for transmitting the intracranial shear waves. This system has to bypass the body's natural protection while keeping a good level of comfort for the human subject. In early brain MRE studies, the vibration transmission was achieved by directly attaching the electromechanical actuators (active drivers) to either a head cradle or a bite bar (passive drivers).[7–10] With the objectives of increased patient comfort and safety, current MRE driver systems in clinical use typically utilize a speaker system located in the MRI equipment room as an active driver, which connects either to a pillow-like passive driver inside the MRI scanner via a pneumatic hose[11] or to a head-rocker unit via a rigid rod.[12] Figure 1A shows an example of a pneumatic active-passive driver system for brain MRE. The active driver located outside the scan room is composed of a waveform generator, an amplifier, and an acoustic speaker. The passive pillow-like driver is positioned under the subject's head in the MRI head coil and inflates/deflates in response to the actuation of the acoustic speaker. Based on our experience, this system is operator-friendly with little patient discomfort.

In brain MRE, the motion is continuously applied at a known frequency using the external driver. Parameters such as the frequency and amplitude of external vibration can be adjusted within appropriate safety limits.[13] Induced wavelength in tissue can be shortened by increasing the vibration frequency, which leads to a greater signal-to-noise ratio (SNR) in stiffness estimation as a result of larger spatial derivatives. However, increasing frequency also increases the attenuation of intracranial shear waves due to the mechanical shielding of

the skull and the viscosity of brain tissue.[14] Consequently, the choice of vibration frequency depends on the best trade-off between these two competing effects. The frequency range reported in human brain MRE literature is between 20 and 150 Hz, with the majority of brain MRE studies are performed in the range of 25–62.5 Hz.[7,8,15–18] A frequency of 60 Hz has been typically used by our group because at that frequency the driver has a high amplitude response while being capable of delivering sufficient shear wave motion deep into the structure of the brain. MRE at multiple frequencies can be performed (either separately or simultaneously) to more completely determine the rheological behavior of brain tissue.[15,19] Besides external driver systems, brain MRE techniques acquired with intrinsic activation have been developed to assess the natural shear waves at a lower frequency (e.g., ~ 1 Hz) that are caused by cardiac motion and blood pulsation.[20–22] Low-frequency MRE is expected to be more sensitive to poroelastic properties of biological tissue.[23]

After the mechanical excitation has been established, a phase-contrast based MR pulse sequence is used to encode the shear wave motion into the MR phase signal using a series of magnetic field gradients called motion encoding gradients (MEG). The underlying physics for MRE motion encoding has been described in the previous publications.[1,24] Basically, synchronized with the applied vibration, application of MEG adds to the spin isochromat (i.e., an ensemble of spins) a phase accrual that is proportional to the displacement vector, and the proportional constant is determined by the MEG strength and duration as well as the phase shift between the mechanical vibration and MEG. It is generally desirable to calculate the phase difference image from two phase images acquired with reversed MEG polarities. In so doing, phase artifacts from the static magnetic field can be removed and the motion encoding efficiency is doubled. In the acquired phase images, the signal of each pixel represents the direction and amount of displacement vector. The phase image that contains the information of the propagating wave is thus called the wave image (Figure 1B). Multiple such images can be acquired at different phase offsets spaced equally over a cycle by adjusting the phase offset between the vibration and MEG. A Fourier transform through time at the driving frequency can then be used to reconstruct the complex-valued shear wave propagation at that frequency.

The most common pulse sequence used for brain MRE is single-shot echo-planar imaging (EPI).[10,11] The single-shot nature of this method makes it very fast. This becomes important when acquiring the full 3-D vector displacement field over the entire brain volume. In our clinical research studies, a high-performance compact 3T scanner[25,26] equipped with a single-shot spin-echo EPI pulse sequence allows acquisition of whole brain coverage with 3 mm^3 isotropic resolution, full 3D vector field (±x, ±y, and ±z) with 8 phase offsets, 60-Hz MRE data in about 3 minutes. Alternative fast acquisition schemes include multislab, multishot spiral MRE to overcome some specific EPI limitations (e.g., limited resolution and high susceptibility artifacts) but requiring off-line reconstruction, which may not fit well into clinical workflow,[27,28] and sample interval modulation-MRE (SLIM-MRE) for fast and optimized 3D wavefield acquisition at the expense of SNR.[29]

Quantitative and qualitative parameters derived from MRE

To obtain the viscoelastic features (e.g., complex shear modulus) of brain tissue from the measured dynamic displacement field, one needs inverse reconstruction algorithms to convert the displacement data to mechanical properties. Generally speaking, the most commonly used inversion methods for brain MRE can be divided into two categories: direct inversion (DI)[30–33] and iterative inversion.[18,34,35] The DI algorithm solves the wave equation locally at each point in the volume to obtain the complex-valued shear modulus. It relies on a set of assumptions including that the tissue is homogeneous and isotropic.[30] In principle, these assumptions violate real brain tissue mechanical properties that include significant heterogeneity and anisotropy. Therefore, the averaging and smoothing effect resulting from this approach presumes some homogeneity in the region of interest, and the estimated shear modulus is considered as an effective shear modulus; however, it can still be useful in quantifying the relative hardness of the tissue of interest. One of the major issues of DI is the high sensitivity of the estimated parameters to noise as the calculation of high order spatial derivatives in DI tends to amplify the noise. Several approaches have been developed to stabilize the results by performing multifrequency inversion[32] or applying the application-specific filters.[36] Iterative inversion (such as nonlinear inversion, NLI) involves minimizing the difference between the measured displacements and a set of displacements generated by a computational model of the system, where an estimate of shear modulus (the unknown property distribution) is iteratively updated until the minimum of the objective function is reached.[35] In contrast to DI, iterative inversion avoids the local homogeneity assumption and deals well with tissue boundaries; however, the reliability of the resulting parameters is highly dependent on accurate modeling of boundary conditions. In addition, the computation time is significantly longer for iterative inversions than DI (several hours versus several seconds), which makes DI more suitable to fit within the clinical workflow. Besides the aforementioned algorithms, an intriguing new direction in inversion approaches is the use of artificial neural networks. A preliminary study has shown that a neural network inversion (NNI) stiffness estimate is more resistant to noise than conventional DI.[37]

Both direct and iterative inversions reconstruct the complex shear modulus G^*, which can be represented by the sum of storage (G') and loss moduli (G''), i.e., $G^* = G' + iG''$. The storage modulus indicates the material's ability to store energy, while the loss modulus is related to the amount of energy loss through viscous processes, and both are frequency dependent. The magnitude of the complex shear modulus ($|G^*|$) is often reported. The phase angle $\varphi = \arctan(G''/G')$, or damping ratio $\xi = G''/2G'$ compare the relative strength of the storage and loss moduli, and are related to the attenuation per wavelength. The commonly reported shear stiffness μ is related to the wave speed squared and can be calculated as $\mu = 2|G^*|^2/(G' + |G^*|)$.[36] It can be thought of as an effective shear modulus, i.e., the shear modulus of a purely elastic object that exhibits the observed wave speed or wavelength at the driving frequency. While stiffness may be convenient to use in the clinical practice to characterize the relative hardness of tissue, complex shear modulus and frequency-dependent viscoelastic parameters provide added value in characterizing the viscoelastic behavior of brain tissue and have been the subject of intense research. For example, multifrequency data can be fitted to a two-parameter viscoelastic model (e.g., springpot model) to provide an estimate of the shear elasticity that describes the solid-fluid behavior of

the tissue and a powerlaw exponent related to the tissue's microstructure.[38] It has been suggested in theory, phantom experiments, and animal and human studies that one could portray the complex interaction of density, geometry, and structure of the underlying mechanical network in biological tissues on a macroscopic voxel scale by using these viscoelastic parameters.[19,38–47] The relationship of specific parameters to the physiological and pathological states of neural tissue will be discussed in more detail later.

Beyond shear stiffness and modulus, many other parameters derived from MRE have great potential to enhance the characterization of disease-related structural changes in human brain. For example, motion information obtained with MRE can be adapted to slip interface imaging (SII) to qualitatively assess the degree of adhesiveness between two adjacent tissue layers, which has significant implications for improving preoperative planning prior to tumor resection.[48–50] It has been reported that the intracranial volumetric strain is sensitive to venous pressure altered by abdominal muscle contraction and to brain dilatation induced by the Valsalva maneuver,[21,51,52] and may have a role in understanding diseases involving pathological pressure alterations such as hydrocephalus. Analysis of the relative skull and brain motion induced by MRE reveals the mechanical coupling of the skull-brain interface,[53] which could provide biofidelity targets for traumatic brain injury (TBI) modeling development and validation, as well as improve the understanding of brain protection mechanisms to facilitate risk management for future injury.

MRE anisotropy measures

The DI inversion that is most commonly used in the clinical environment assumes brain isotropy to simplify analysis and interpretation of MRE measurement while still making a meaningful physical interpretation of the measured global stiffness. However, brain white matter tissue is highly anisotropic due to its specific organization in bundles of myelinated axonal fibers running in parallel; therefore, the stiffness is not necessarily the same in all directions. It has been reported that the estimated brain mechanical properties exhibit a distinct difference in highly aligned white matter tracts under different excitation directions where waves may travel at different angles to the fiber direction.[54] Many approaches have been investigated to study the effect of anisotropy on brain stiffness estimates. For example, several MRE studies based on transverse isotropic models with controlled excitation modes have been performed to estimate both shear and tensile anisotropy on numerical and physical phantoms, and *ex vivo* biological tissues.[55–58] Slow and fast shear waves were identified and the corresponding wave speeds were calculated to estimate the shear modulus, shear anisotropy, and tensile anisotropy. While these studies focus on transversely isotropic materials where the fibers are assumed to be fairly straight, the curvature of neural fibers in the brain makes a direct application of this approach somewhat difficult.

As an alternative, waveguide elastography (WGE) was proposed to assess the anisotropic elasticity tensor of nerve fibers (such as the corticospinal tracts, CSTs) based on an orthotropic material model with nine independent elastic constants.[59,60] This method utilizes diffusion tensor imaging (DTI) to determine the fiber orientation of white matter, and then a spatial-spectral filter in combination with a Helmholtz decomposition is applied to the MRE measurements to separate the waves into longitudinal and transverse components

propagating within a local reference frame along the fibers. Due to this process, the equations of motion decouple allowing for each of the 9 orthotropic stiffness coefficients to be solved independently. Furthermore, Romano *et al.* introduced an analysis method called mixed-model inversions (MMI) to simultaneously evaluate the stiffness parameters of both isotropic and anisotropic regions of the brain.[61] Both isotropic and anisotropic inversions are performed within the human brain using a data-driven delineation method. Fractional anisotropy (FA) calculated from DTI is utilized as a thresholding metric to differentiate between isotropic (FA < 0.2) and anisotropic (FA ≥ 0.2) regions.[62] For FA < 0.2, the isotropic inversion algorithm is implemented,[63] while for FA ≥ 0.2, the anisotropic inversion algorithm is implemented.[60] While these anisotropic inversion approaches have only recently been established and no current consensus has been reached, there is a great potential for applying them to evaluate neurodegenerative diseases.

Applications of Brain MRE

MRE in neural tissues

The brain mechanical properties measured from MRE can be influenced by a variety of factors such as cell density, extracellular matrix (ECM) density, and neural network structure and integrity that constitute the complicated microstructure of neural tissue. Besides that, it is clear that the estimated mechanical parameters are dependent on the choice of MRE imaging parameters and inversion algorithms. This dependency complicates the direct comparison of MRE results among different studies. Despite some variations, there is broad agreement that (1) human brain tissue is soft with global shear stiffness of 1–3.5 kPa in the commonly used frequency range of 50–60 Hz and very soft (~ 0.5 kPa) at lower frequencies (< 20 Hz),[2] exhibiting viscoelastic behavior; (2) white matter is stiffer than gray matter,[14,18,64,65] which is microstructurally plausible as white matter consists primarily of myelinated axons, that act as a network of biopolymer filaments, while gray matter is largely composed of neuronal cell bodies, dendrites, and unmyelinated axons;[66,67] and (3) white matter is more viscous than gray matter,[14,18,64,65] with the complex microstructural interactions in the network of white matter probably causing the higher attenuation.[39,40] MRE characterizes the intact brain tissue noninvasively and thus can complement other measurements performed on the tissue level[68] and cellular level[69] about gray and white matter stiffness in the current brain mechanical literature.

Within white matter, the number of axons, axonal density, axon size, packing, myelin thickness, etc. vary between different tracts. With advancements in the brain MRE acquisition and post-processing techniques, one now has the opportunity to measure the regional variation in brain stiffness between specific structural components. This has been demonstrated in several MRE studies of healthy subjects, including Guo *et al.* who reported a significant stiffness contrast between several fine structures such as corpus callosum genu (CCG), thalamus, and the head of the caudate nucleus (HCN) with the highest stiffness in CCG and lowest in HCN.[17] Johnson *et al.* reported that the corpus callosum (CC) exhibits greater stiffness and less viscous damping than the corona radiata (CR);[18,27] they also detected viscoelastic variations in different subcortical gray matter structures including the amygdala, hippocampus, caudate, putamen, pallidum, and thalamus.[70] Murphy *et al.*

characterized the regional stiffness within the lobes of the brain and the cerebellum and found that stiffness in parietal lobe and cerebellum were significantly lower than other regions,[16] consistent with Zhang *et al.*'s and Johnson *et al.*'s studies that the cerebellum appears to be softer compared to the central cerebrum.[28,64] Although the absolute material property values vary across different MRE research groups due to the heterogeneity of the acquisition and inversion methodologies, highly repeatable measures can be achieved within consistent acquisition and inversion pipelines. Using a 3-mm isotropic resolution EPI sequence and a brain-specific DI inversion pipeline, MRE estimates were reproducible in 10 healthy subjects with typical errors of less than 1% for global brain stiffness and less than 2% for the brain lobes.[16] In Johnson *et al.*'s study utilizing a spiral sequence and nonlinear inversion (NLI) algorithm, the coefficient of variation was found to be below 7% for all measured small brain regions through repeated examinations on a single volunteer.[70] However, much effort is still needed to construct a reliable neuroanatomy atlas of brain mechanics in terms of higher resolution and cross-validation with different brain MRE techniques.

In addition to quantifying regional stiffness variations in the living brain, MRE can be used to gain neurobiological insight into the effects of age and gender on the brain. A progressive decrease in brain stiffness with healthy aging has been noted.[38,71–73] Investigators found that global brain tissue softens on the order of 0.3–1% per year, and the change rate is three times greater than the rate of volume decrease.[38,71] The changes are also dependent on regions, with the significant linear correlation between age and brain stiffness observed in the cerebrum and 4 brain lobes but not in cerebellum and sensory-motor regions.[72] Another study compared a group of young individuals, with a mean age of 25.2 years, to a group of older individuals with a mean age of 69.4 years and reported a regional stiffness reduction in cerebrum, amygdala, caudate, pallidum, putamen, and thalamus, as well as volume reduction but no change in damping ratio in older adults.[71] An illustration of brain softening with aging is shown in Figure 2. No MRE data has been reported with respect to the developing brain, except for a review article discussing the potential of brain MRE in developmental neuroimaging.[74] Unlike aging, the MRE findings of gender-dependent differences in brain stiffness are somewhat controversial. Our group found female occipital and temporal lobes to be stiffer than males of the same age,[72] which is consistent with Sack *et al.*'s study which suggested that female brains were stiffener than their male counterparts throughout the brain.[38] However, this same group reported no significant gender effect in a later study.[71] Histological work has suggested the potential mechanisms of reduced white matter integrity with aging,[75–77] and differences in the number of neural and glial cells with gender.[78] It is possible that MRE measurements are sensitive to these histological properties. Yet, the effects of age and gender on brain mechanical properties and the correlation to histological alterations remains an open area of investigation.

Given that brain structure and function are closely related, recent work has suggested that brain MRE could also be used to characterize changes in tissue viscoelasticity associated with cognitive function and behavior. A strong relationship between damping ratio and relational memory performance has been reported in the human hippocampus during a spatial reconstruction task in a group of young healthy adults.[79] Better aerobic fitness as measured by VO_2max and better relational memory performance were associated with a

lower hippocampal damping ratio, while such a relationship was not found with hippocampal volume (Figure 3).[80] A link between exercise-related improvements in cognition and underlying hippocampal viscoelasticity in patients with multiple sclerosis (MS) has also been reported.[81] This suggests a possible new direction to examine functional performance with MRE-derived viscoelastic properties in order to evaluate the change in brain structure and cognitive function, as well as to understand the differences in brain structures relating to individual differences in cognitive patterns.

MRE in intracranial tumors

Surgery is the primary treatment for intracranial tumors that can be removed without causing severe functional damage. Brain MRE has for the first time demonstrated the ability to characterize preoperatively tumor consistency and adherence to adjacent normal brain tissue. This information offers improved surgical planning and determination of surgical risk. For example, resecting soft meningiomas are relatively easily evacuated with suction, but hard tumors often require sharp dissection and piecemeal removal with ultrasonic aspirators. Moreover, non-adherent tumors where a slip interface is present relative to surrounding healthy tissue are easier and safer to remove than tumors that are adherent to adjacent brain tissue. To have this information available preoperatively can influence surgical planning and lead to a safer and more easily tolerated surgical procedure. MRE assessment of tumor consistency was initially reported with a high accuracy by correlating MRE measured stiffness with a haptic assessment by the surgeon in mixed solid brain tumors.[7] Similar findings were shown in another MRE study compared with intraoperative consistency grading.[82] Two MRE studies of meningiomas published by our group further demonstrated the excellent agreement between MRE-assessed stiffness and a 5-point scale graded intraoperative consistency.[83,84] Tumor stiffness prediction using MRE has performed best in larger tumors that were not overly vascular. However, characterizing the consistency of tumors that are vascular, heterogeneous, and small (< 3.5 cm) has been challenging, requiring investigation with further improvements including higher spatial resolution.

With regard to tumor adherence, slip interface imaging (SII) was developed to qualitatively predict the degree of tumor-brain adhesion. In response to an applied shear motion with MRE, a tumor without adhesion will slip at a tumor–brain boundary compared to an adherent tumor. As a result, the shear wave propagating through the brain becomes discontinuous at the tumor-brain boundary with a relatively large spatial gradient of the displacement. A slip interface can be detected by SII as low signals on shear line images and high octahedral shear strain (OSS) values along the tumor-brain interface. Yin *et al*. have demonstrated the value of SII in predicting tumor adherence in vestibular schwannomas[48] and meningiomas,[49] using findings at surgery as the reference standard, in which the SII prediction has a high degree of correlation with the intraoperative assessment of tumor adherence. An illustration of MRE and SII assessments of meningiomas is highlighted in Figure 4, in which two cases are shown: a firm and non-adherent tumor, and a soft and adherent tumor. Despite improved prediction accuracy with normalizing OSS to the wave amplitude,[49] SII prediction is still challenged by non-slip factors including modulus contrast, wavelength variations, and wave scattering at the interface.[85,86]

Another useful and potential application of brain MRE is the identification of tumor subtype and grade, as tumors with higher grade malignancy are more likely to be softer and less viscous despite significant overlap of values.[87–90] A detailed discussion of the use of brain MRE in tumor differentiation will be provided elsewhere in this Special Issue ("*Quantifying Tumor Stiffness with MRE, the Role of Mechanical Properties for Detection, Characterization, and Treatment Stratification in Oncology*").

MRE in Alzheimer's and Non-Alzheimer forms of degenerative dementia

Brain MRE provides direct insights into the brain mechanical characteristics of patients with different forms of dementia, improving our comprehension of the underlying pathological processes of dementia. MRE studies of patients with Alzheimer's disease (AD) have demonstrated changes in global and regional stiffness associated with progression of the disease.[11] In addition to a decrease in global brain stiffness, AD patients show a specific pattern of regional softening involving the frontal, parietal, and temporal lobes.[91] Interestingly, stiffness was observed to correlate with the severity of AD nonlinearly and non-monotonically, which correlated with measures of connectivity in the default mode network on resting-state functional MRI. Gerischer *et al.* showed reduced stiffness globally and within the hippocampus, as well as reduced hippocampal viscosity in patients with AD;[92] they also showed an improved diagnostic accuracy by combining MRE with MR diffusion and volume measures, suggesting the advantage of multi-modality MRI in AD diagnosis. Findings from the animal studies are concordant with those described in patients. These results further support the conclusion that stiffness changes may be due to ECM degradation, cell loss, neurodegeneration or some combination of these processes, rather than amyloid deposition alone.[44,93,94] It should be noted that the differences observed with MRE measures compared to the changes in volume measures suggest that MRE measures provide more sensitive information about neural tissue organization or degeneration than to volume measures, or may suggest that MRE is providing information that is independent or related to volume in a complex way.

MRE analysis of regional stiffness changes has demonstrated the potential value of MRE in the differentiation of different types of dementia (Figure 5). A recent study compared measures of stiffness between patients with AD, frontotemporal dementia (FTD), dementia with Lewy bodies (DLB), normal pressure hydrocephalus (NPH), and subjects without dementia.[95] Compared with AD patients, patients with FTD had significantly lower stiffness values in the frontal and temporal lobes but not the parietal lobes.[96] Unlike AD and FTD, patients with DLB did not show any significant changes in the stiffness of any brain regions. Patients with NPH showed an increase in stiffness in parietal, occipital, and sensory-motor regions.[97,98] However, different NPH findings have been reported in other studies, where the global softening of brain tissue and the decreased powerlaw exponent was detected.[42,99] The disparity in stiffness measures of NPH warrants further investigation of the underlying mechanisms. MRE studies with Parkinson's disease (PD) have reported a reduced brain viscoelasticity in PD patients,[100,101] which has also been shown in MRE studies using mouse models of PD.[102,103] A detailed regional analysis separated PD from progressive supranuclear palsy (PSP) - two diseases that share similar clinical symptoms but with

different neuropathology. The reduction of brain viscoelasticity was found to be stronger in PSP than PD with an enhanced reduction in the mesencephalic region.[100,101]

Overall, degenerative diseases associated with the AD or non-AD types of dementia represent important challenges in terms of diagnosis and differentiation and are increasing in importance with the aging population. Therefore, further development, including combining with different methods of neuroimaging, will assist in the diagnosis of different forms of dementia, hopefully in the early stages.

MRE in demyelination and neuroinflammatory disorders

Multiple sclerosis (MS) is the most common disabling neurological condition and is characterized by the axonal loss and demyelination lesions in the central nervous system. MRE has been used in MS to provide insights into the mechanisms of damage in terms of mechanical alterations. In particular, MRE studies of MS have consistently demonstrated that stiffness is reduced in MS patients, presumably due to demyelination and inflammation resulting from widespread tissue integrity degradation. The first clinical pilot study of brain MRE observed significantly reduced global brain parenchymal viscoelasticity in mild relapsing-remitting (RR) MS patients compared to matched controls, while the springpot model-related structure-geometry parameter remained unchanged.[104] Furthermore, there is evidence that primary and secondary chronic-progressive (PP and SP) MS showed a pronounced reduction of the cerebral shear elasticity compared to early RR-MS as well as a significant decrease in the same structure-geometry parameter, indicating an alteration in the geometry of the cerebral mechanical network due to chronic neuroinflammation.[43] Patients with clinically isolated syndrome (CIS), referring to the first clinical onset of potential MS, exhibited similar brain viscoelastic behavior as other subforms of MS – a softening of brain parenchyma with no significant change in the structure-geometry parameter.[105] With regard to changes of MRE-derived measurements over time, Figure 6 summarizes the clinical MRE findings in three stages of MS. In a recent pilot study of MS, hippocampal viscoelasticity was found to be correlated with learning and memory improvements with training,[81] suggesting the potential of MRE to be used as a treatment outcome measure. In addition to MS, accelerated softening of the brain parenchyma was also demonstrated in another autoimmune inflammatory disease, neuromyelitis optica spectrum disorder (NMOSD).[106]

A further confirmation of these clinical results came from MRE-pathological correlation studies in *ex vivo* or *in vivo* MS preclinical models. In a mouse model of reversible toxic demyelination, decreased brain viscoelasticity was found to be directly associated with both demyelination and ECM degradation; such a change was also reversible after remyelination.[107] This relationship between brain stiffness and demyelination can also be explained by an *ex vivo* investigation of the bovine brain in which brain stiffness, particularly cerebral white matter stiffness, was directly proportional to the local myelin content.[108] MRE characterization of an experimental autoimmune encephalomyelitis (EAE) model revealed a clear correlation between viscoelastic tissue alteration and the magnitude of perivascular T cell infiltration, demonstrating the sensitivity of MRE to early acute neuroinflammation.[109] The follow-up study of a chronic EAE model confirmed a further relationship between cellular inflammation and EAE-related decreased in brain stiffness.[110] Although the

mechanical signatures of demyelination and inflammation appear to overlap, the preclinical and clinical correlations reported so far suggest MRE can be used as a potential biomarker to quantify the onset of MS progression.

MRE in amyotrophic lateral sclerosis

Amyotrophic lateral sclerosis (ALS) is a progressive neurodegenerative disorder that affects the nerves in the brain and spinal cord secondarily. MRE was employed in ALS, with promising results, by Romano *et al.*, who used waveguide elastography (WGE) to study the changes of anisotropic stiffness parameters within the corticospinal tracts (CSTs) in ALS patients.[111] DTI was performed to determine the fiber pathways of the CSTs, and WGE was applied to reconstruct anisotropic stiffness values. Two anisotropic shear moduli, polarized parallel (C_{44}) and perpendicular (C_{66}) to the CSTs, were found to be significantly reduced in ALS patients compared to the controls (Figure 7). The reduction in stiffness of the CSTs in the ALS patients may be attributed to Wallerian degeneration which leads to a disintegration of the axonal skeleton and membrane followed by a degradation of the myelin sheath and infiltration by macrophages.[107,112,113] These results suggest that anisotropic stiffness parameters may provide valuable and complementary information about brain mechanical behavior where tissue anisotropy is altered as a result of neurodegeneration.

MRE in traumatic brain injury

A potentially interesting application of MRE is the study of traumatic brain injury (TBI) since the concussion and other types of TBI may involve significant deformation and injury of brain tissue resulting in possible alterations of mechanical behavior. In Romano *et al.*'s pilot MRE studies,[61,114] the mixed model inversion (MMI) was applied to patients with moderate to severe TBI, and alterations to the brain structures and decreased brain stiffness as a result of insult were found as illustrated in Figure 8. As characterized by DTI, spherical shapes indicate isotropic regions, while the ellipsoidal shapes indicate anisotropic regions. When compared to the healthy control, the post-traumatic changes within the frontal lobe of the TBI patient replaced the anisotropic forceps minor with an isotropic lesion, consisting of glial scarring and encephalomalacia, which led to the reduced FA and shear stiffness. Similar trends were also found in other MRE studies using preclinical TBI models. In a controlled cortical impact injury (CCI) mouse model, reduced shear stiffness was reported in injured brain regions compared with the unaffected controls.[115] The same group further investigated the long-term viscoelastic properties of the injured brain tissue *in vivo* after CCI and observed a significant drop in the stiffness of the impacted region immediately following the injury and an increase of the stiffness after the injury.[116] Furthermore, recent work investigating the longitudinal and regional stiffness changes in a weight-drop injured mouse model, using an indentation test, found an increase-decrease-increase pattern in stiffness change over time at the tissue level and correlated it with morphological and biological changes at the cellular level.[117]

Another promising application lies in the understanding of the TBI biomechanics by quantifying the skull-brain coupling, i.e., the motion (or shear stress) transmission and attenuation from the skull to the brain.[14,53,118] The skull has been found to act as a low-pass filter, and the skull-brain interface significantly attenuates and delays transmission of motion

from the skull to the brain. The transmission and attenuation coefficients might be different between healthy and TBI subjects due to the disruption of normal skull-brain coupling as a result of the head impact. Moreover, given that the mechanical behavior of brain tissue is very difficult to model, MRE could potentially provide biofidelity targets for TBI modeling development and validation. Despite the preliminary nature of these investigations, the results are encouraging and suggesting that MRE may provide a window into this complex structural system to improve our understanding of TBI biomechanics.

Challenges for the Future

Brain MRE has the potential to provide information about neural structure and function under various physiologic and pathologic conditions noninvasively and *in vivo*. But as mentioned throughout this review, two of the biggest problems are the lack of consistency across studies and the lack of disease specificity for the MRE measures that are employed.

As discussed above in detail, the lack of consistency across studies is in part due to the widely variable methodologies used for data acquisition, processing, and analysis, but in part also due to the heterogeneous nature of brain disorders themselves. Multicenter serial studies offer the opportunity for standardization in clinical trials. MRE images usually have lower image quality compared to other conventional MR images due to image quality issues like distortion, noise and low resolution, which can arise from the use of faster image acquisition, such as EPI. As imaging acquisition techniques continue to improve and inversion reconstruction techniques are optimized, higher SNR MRE images will improve the precision of our measurements.[26,65,119,120]

Another area that will likely to be the focus of future research involves the biology of MRE. That is, while the vast majority of MRE studies demonstrated brain viscoelastic anomalies, questions still remain – what are we actually measuring, how specific are our measurements, and how are our measurements relevant to the brain structure and function? It is evident that MRE measurements are sensitive to the histological properties associated with degeneration, ECM remodeling, inflammation, perfusion[121], edema, intracranial pressure, and cellular mechanisms. However, similar to the non-specific issues that plague much of the rest of quantitative MRI, there are many possible reasons for an increase or decrease of the brain viscoelasticity in a particular disease. A solid link between MRE findings and histological or immunohistochemical changes is currently lacking. Hence, an important issue that requires further investigation is how to improve the low specificity of current MRE methods in describing the nature of observed pathology, involving using numerical, physical, and preclinical validation models.

Concluding Remarks

In summary, brain MRE is a quantitative method that gives direct insight into the macroscopic and voxel-averaged microscopic mechanical properties of tissues. MRE is the only approach available today to assess brain mechanical properties noninvasively. MRE has improved both our understanding of diseases and our ability to detect and monitor pathological changes in research and clinical settings. When combined with the development

of high-resolution scans and methodological improvements, the capabilities of MRE will continue to expand.

References

1. Muthupillai R, Lomas DJ, Rossman PJ, et al. Magnetic resonance elastography by direct visualization of propagating acoustic strain waves. Science. 1995; 269(5232):1854–1857. [PubMed: 7569924]
2. Hiscox LV, Johnson CL, Barnhill E, et al. Magnetic resonance elastography (MRE) of the human brain: technique, findings and clinical applications. Phys Med Biol. 2016; 61(24):R401–R437. [PubMed: 27845941]
3. Murphy MC, Huston J, Ehman RL. MR elastography of the brain and its application in neurological diseases. NeuroImage. 2017; doi: 10.1016/j.neuroimage.2017.10.008
4. Ophir J, Cespedes I, Ponnekanti H, et al. Elastography: a quantitative method for imaging the elasticity of biological tissues. Ultrason Imaging. 1991; 13(2):111–134. [PubMed: 1858217]
5. Parker KJ, Doyley MM, Rubens DJ. Imaging the elastic properties of tissue: the 20 year perspective. Phys Med Biol. 2011; 56(1):R1–R29. [PubMed: 21119234]
6. Doyley MM, Parker KJ. Elastography: general principles and clinical applications. Ultrasound clinics. 2014; 9(1):1–11. [PubMed: 24459461]
7. Xu L, Lin Y, Han JC, et al. Magnetic resonance elastography of brain tumors: preliminary results. Acta Radiol. 2007; 48(3):327–330. [PubMed: 17453505]
8. Green MA, Bilston LE, Sinkus R. In vivo brain viscoelastic properties measured by magnetic resonance elastography. NMR Biomed. 2008; 21(7):755–764. [PubMed: 18457350]
9. Kruse SA, Rose GH, Glaser KJ, et al. Magnetic resonance elastography of the brain. Neuroimage. 2008; 39(1):231–237. [PubMed: 17913514]
10. Hamhaber U, Sack I, Papazoglou S, et al. Three-dimensional analysis of shear wave propagation observed by in vivo magnetic resonance elastography of the brain. Acta Biomater. 2007; 3(1):127–137. [PubMed: 17067861]
11. Murphy MC, Huston J 3rd, Jack CR Jr, et al. Decreased brain stiffness in Alzheimer's disease determined by magnetic resonance elastography. J Magn Reson Imaging. 2011; 34(3):494–498. [PubMed: 21751286]
12. Sack I, Beierbach B, Hamhaber U, et al. Non-invasive measurement of brain viscoelasticity using magnetic resonance elastography. NMR Biomed. 2008; 21(3):265–271. [PubMed: 17614101]
13. Ehman EC, Rossman PJ, Kruse SA, et al. Vibration safety limits for magnetic resonance elastography. Phys Med Biol. 2008; 53(4):925–935. [PubMed: 18263949]
14. Clayton EH, Genin GM, Bayly PV. Transmission, attenuation and reflection of shear waves in the human brain. J R Soc Interface. 2012; 9(76):2899–2910. [PubMed: 22675163]
15. Klatt D, Hamhaber U, Asbach P, et al. Noninvasive assessment of the rheological behavior of human organs using multifrequency MR elastography: a study of brain and liver viscoelasticity. Phys Med Biol. 2007; 52(24):7281–7294. [PubMed: 18065839]
16. Murphy MC, Huston J 3rd, Jack CR Jr, et al. Measuring the characteristic topography of brain stiffness with magnetic resonance elastography. PLoS ONE. 2013; 8(12):e81668. [PubMed: 24312570]
17. Guo J, Hirsch S, Fehlner A, et al. Towards an elastographic atlas of brain anatomy. PLoS ONE. 2013; 8(8):e71807. [PubMed: 23977148]
18. Johnson CL, McGarry MD, Gharibans AA, et al. Local mechanical properties of white matter structures in the human brain. Neuroimage. 2013; 79:145–152. [PubMed: 23644001]
19. Dittmann F, Hirsch S, Tzschätzsch H, et al. In vivo wideband multifrequency MR elastography of the human brain and liver. Magn Reson Med. 2016; 76(4):1116–1126. [PubMed: 26485494]
20. Weaver JB, Pattison AJ, McGarry MD, et al. Brain mechanical property measurement using MRE with intrinsic activation. Phys Med Biol. 2012; 57(22):7275–7287. [PubMed: 23079508]

21. Hirsch S, Klatt D, Freimann F, et al. In vivo measurement of volumetric strain in the human brain induced by arterial pulsation and harmonic waves. Magn Reson Med. 2013; 70(3):671–683. [PubMed: 23008140]
22. Zorgani A, Souchon R, Dinh AH, et al. Brain palpation from physiological vibrations using MRI. Proc Natl Acad Sci USA. 2015; 112(42):12917–12921. [PubMed: 26438877]
23. McGarry MD, Johnson CL, Sutton BP, et al. Suitability of poroelastic and viscoelastic mechanical models for high and low frequency MR elastography. Med Phys. 2015; 42(2):947–957. [PubMed: 25652507]
24. Muthupillai R, Rossman PJ, Lomas DJ, et al. Magnetic resonance imaging of transverse acoustic strain waves. Magn Reson Med. 1996; 36(2):266–274. [PubMed: 8843381]
25. Tan ET, Lee SK, Weavers PT, et al. High slew-rate head-only gradient for improving distortion in echo planar imaging: Preliminary experience. J Magn Reson Imaging. 2016; 44(3):653–664. [PubMed: 26921117]
26. Weavers PT, Shu Y, Tao S, et al. Technical Note: Compact three-tesla magnetic resonance imager with high-performance gradients passes ACR image quality and acoustic noise tests. Med Phys. 2016; 43(3):1259–1264. [PubMed: 26936710]
27. Johnson CL, McGarry MD, Van Houten EE, et al. Magnetic resonance elastography of the brain using multishot spiral readouts with self-navigated motion correction. Magn Reson Med. 2013; 70(2):404–412. [PubMed: 23001771]
28. Johnson CL, Holtrop JL, McGarry MD, et al. 3D multislab, multishot acquisition for fast, whole-brain MR elastography with high signal-to-noise efficiency. Magn Reson Med. 2014; 71(2):477–485. [PubMed: 24347237]
29. Klatt D, Johnson CL, Magin RL. Simultaneous, multidirectional acquisition of displacement fields in magnetic resonance elastography of the in vivo human brain. J Magn Reson Imaging. 2015; 42(2):297–304. [PubMed: 25425147]
30. Oliphant TE, Manduca A, Ehman RL, et al. Complex-valued stiffness reconstruction for magnetic resonance elastography by algebraic inversion of the differential equation. Magn Reson Med. 2001; 45(2):299–310. [PubMed: 11180438]
31. Papazoglou S, Hamhaber U, Braun J, et al. Algebraic Helmholtz inversion in planar magnetic resonance elastography. Phys Med Biol. 2008; 53(12):3147–3158. [PubMed: 18495979]
32. Papazoglou S, Hirsch S, Braun J, et al. Multifrequency inversion in magnetic resonance elastography. Phys Med Biol. 2012; 57(8):2329–2346. [PubMed: 22460134]
33. Hirsch S, Guo J, Reiter R, et al. MR elastography of the liver and the spleen using a piezoelectric driver, single-shot wave-field acquisition, and multifrequency dual parameter reconstruction. Magn Reson Med. 2014; 71(1):267–277. [PubMed: 23413115]
34. Van Houten EE, Miga MI, Weaver JB, et al. Three-dimensional subzone-based reconstruction algorithm for MR elastography. Magn Reson Med. 2001; 45(5):827–837. [PubMed: 11323809]
35. McGarry MD, Van Houten EE, Johnson CL, et al. Multiresolution MR elastography using nonlinear inversion. Med Phys. 2012; 39(10):6388–6396. [PubMed: 23039674]
36. Manduca A, Oliphant TE, Dresner MA, et al. Magnetic resonance elastography: non-invasive mapping of tissue elasticity. Med Image Anal. 2001; 5(4):237–254. [PubMed: 11731304]
37. Murphy MC, Manduca A, Trzasko JD, et al. Artificial neural networks for stiffness estimation in magnetic resonance elastography. Magn Reson Med. 2017; doi: 10.1002/mrm.27019
38. Sack I, Beierbach B, Wuerfel J, et al. The impact of aging and gender on brain viscoelasticity. Neuroimage. 2009; 46(3):652–657. [PubMed: 19281851]
39. Guo J, Posnansky O, Hirsch S, et al. Fractal network dimension and viscoelastic powerlaw behavior: II. An experimental study of structure-mimicking phantoms by magnetic resonance elastography. Phys Med Biol. 2012; 57(12):4041–4053. [PubMed: 22674199]
40. Posnansky O, Guo J, Hirsch S, et al. Fractal network dimension and viscoelastic powerlaw behavior: I. A modeling approach based on a coarse-graining procedure combined with shear oscillatory rheometry. Phys Med Biol. 2012; 57(12):4023–4040. [PubMed: 22674184]
41. Clayton EH, Garbow JR, Bayly PV. Frequency-dependent viscoelastic parameters of mouse brain tissue estimated by MR elastography. Phys Med Biol. 2011; 56(8):2391–2406. [PubMed: 21427486]

42. Freimann FB, Streitberger KJ, Klatt D, et al. Alteration of brain viscoelasticity after shunt treatment in normal pressure hydrocephalus. Neuroradiology. 2012; 54(3):189–196. [PubMed: 21538046]
43. Streitberger KJ, Sack I, Krefting D, et al. Brain viscoelasticity alteration in chronic-progressive multiple sclerosis. PLoS One. 2012; 7(1):e29888. [PubMed: 22276134]
44. Freimann FB, Muller S, Streitberger KJ, et al. MR elastography in a murine stroke model reveals correlation of macroscopic viscoelastic properties of the brain with neuronal density. NMR Biomed. 2013; 26(11):1534–1539. [PubMed: 23784982]
45. Juge L, Petiet A, Lambert SA, et al. Microvasculature alters the dispersion properties of shear waves--a multi-frequency MR elastography study. NMR Biomed. 2015; 28(12):1763–1771. [PubMed: 26768491]
46. Lambert SA, Näsholm SP, Nordsletten D, et al. Bridging three orders of magnitude: multiple scattered waves sense fractal microscopic structures via dispersion. Phys Rev Lett. 2015; 115(9): 094301. [PubMed: 26371655]
47. Testu J, McGarry MDJ, Dittmann F, et al. Viscoelastic power law parameters of in vivo human brain estimated by MR elastography. J Mech Behav Biomed Mater. 2017; 74:333–341. [PubMed: 28654854]
48. Yin Z, Glaser KJ, Manduca A, et al. Slip interface imaging predicts tumor-brain adhesion in vestibular schwannomas. Radiology. 2015; 277(2):507–517. [PubMed: 26247776]
49. Yin Z, Hughes JD, Glaser KJ, et al. Slip interface imaging based on MR-elastography preoperatively predicts meningioma–brain adhesion. J Magn Reson Imaging. 2017; 46(4):1007–1016. [PubMed: 28194925]
50. Mariappan YK, Glaser KJ, Manduca A, et al. Cyclic motion encoding for enhanced MR visualization of slip interfaces. J Magn Reson Imaging. 2009; 30(4):855–863. [PubMed: 19787735]
51. Hirsch S, Beyer F, Guo J, et al. Compression-sensitive magnetic resonance elastography. Phys Med Biol. 2013; 58(15):5287–5299. [PubMed: 23852144]
52. Mousavi SR, Fehlner A, Streitberger K-J, et al. Measurement of in vivo cerebral volumetric strain induced by the Valsalva maneuver. J Biomech. 2014; 47(7):1652–1657. [PubMed: 24656483]
53. Badachhape AA, Okamoto RJ, Durham RS, et al. The relationship of three-dimensional human skull motion to brain tissue deformation in magnetic resonance elastography studies. J Biomech Eng. 2017; 139(5)doi: 10.1115/1111.4036146
54. Anderson AT, Van Houten EEW, McGarry MDJ, et al. Observation of direction-dependent mechanical properties in the human brain with multi-excitation MR elastography. J Mech Behav Biomed Mater. 2016; 59:538–546. [PubMed: 27032311]
55. Tweten DJ, Okamoto RJ, Schmidt JL, et al. Estimation of material parameters from slow and fast shear waves in an incompressible, transversely isotropic material. J Biomech. 2015; 48(15):4002–4009. [PubMed: 26476762]
56. Schmidt JL, Tweten DJ, Benegal AN, et al. Magnetic resonance elastography of slow and fast shear waves illuminates differences in shear and tensile moduli in anisotropic tissue. J Biomech. 2016; 49(7):1042–1049. [PubMed: 26920505]
57. Tweten DJ, Okamoto RJ, Bayly PV. Requirements for accurate estimation of anisotropic material parameters by magnetic resonance elastography: A computational study. Magn Reson Med. 2017; 78(6):2360–2372. [PubMed: 28097687]
58. Schmidt JL, Tweten DJ, Badachhape AA, et al. Measurement of anisotropic mechanical properties in porcine brain white matter ex vivo using magnetic resonance elastography. J Mech Behav Biomed Mater. 2018; 79:30–37. [PubMed: 29253729]
59. Romano AJ, Abraham PB, Rossman PJ, et al. Determination and analysis of guided wave propagation using magnetic resonance elastography. Magn Reson Med. 2005; 54(4):893–900. [PubMed: 16155879]
60. Romano A, Scheel M, Hirsch S, et al. In vivo waveguide elastography of white matter tracts in the human brain. Magn Reson Med. 2012; 68(5):1410–1422. [PubMed: 22252792]
61. Romano A, Szymczak W, Okamoto R. , et al. National Capital Area Traumatic Brain Injury Symposium. National Institutes of Health; Bethesda, MD, USA: 2016. Traumatic brain injury

studies using magnetic resonance elastography, diffusion tensor imaging, and mixed isotropic and anisotropic inversions.

62. Wakana S, Nagae-Poetscher LM, Jiang H, et al. Macroscopic orientation component analysis of brain white matter and thalamus based on diffusion tensor imaging. Magn Reson Med. 2005; 53(3):649–657. [PubMed: 15723403]
63. Romano A, Bucaro J, Ehman R, et al. Evaluation of a Material Parameter Extraction Algorithm Using MRI-Based Displacement Measurements. IEEE Trans Ultrason, Ferroelect, Freq. 2000; 47(6):1575–1581.
64. Zhang J, Green MA, Sinkus R, et al. Viscoelastic properties of human cerebellum using magnetic resonance elastography. J Biomech. 2011; 44(10):1909–1913. [PubMed: 21565346]
65. Braun J, Guo J, Lutzkendorf R, et al. High-resolution mechanical imaging of the human brain by three-dimensional multifrequency magnetic resonance elastography at 7T. Neuroimage. 2014; 90:308–314. [PubMed: 24368262]
66. Budday S, Steinmann P, Kuhl E. Physical biology of human brain development. Front Cell Neurosci. 2015; 9:257. [PubMed: 26217183]
67. Holland MA, Miller KE, Kuhl E. Emerging brain morphologies from axonal elongation. Ann Biomed Eng. 2015; 43(7):1640–1653. [PubMed: 25824370]
68. Budday S, Nay R, de Rooij R, et al. Mechanical properties of gray and white matter brain tissue by indentation. J Mech Behav Biomed Mater. 2015; 46:318–330. [PubMed: 25819199]
69. Christ AF, Franze K, Gautier H, et al. Mechanical difference between white and gray matter in the rat cerebellum measured by scanning force microscopy. J Biomech. 2010; 43(15):2986–2992. [PubMed: 20656292]
70. Johnson CL, Schwarb HDJ, McGarry M, et al. Viscoelasticity of subcortical gray matter structures. Hum Brain Mapp. 2016; 37(12):4221–4233. [PubMed: 27401228]
71. Sack I, Streitberger K-J, Krefting D, et al. The influence of physiological aging and atrophy on brain viscoelastic properties in humans. PLoS ONE. 2011; 6(9):e23451. [PubMed: 21931599]
72. Arani A, Murphy MC, Glaser KJ, et al. Measuring the effects of aging and sex on regional brain stiffness with MR elastography in healthy older adults. Neuroimage. 2015; 111:59–64. [PubMed: 25698157]
73. Hiscox LV, Johnson CL, McGarry MDJ, et al. High-resolution magnetic resonance elastography reveals differences in subcortical gray matter viscoelasticity between young and healthy older adults. Neurobiol Aging. 2018; 65:158–167. [PubMed: 29494862]
74. Johnson CL, Telzer EH. Magnetic resonance elastography for examining developmental changes in the mechanical properties of the brain. Dev Cogn Neurosci. 2017; doi: 10.1016/j.dcn.2017.08.010
75. Tang Y, Nyengaard JR, Pakkenberg B, et al. Age-induced white matter changes in the human brain: a stereological investigation. Neurobiol Aging. 1997; 18(6):609–615. [PubMed: 9461058]
76. Marner L, Nyengaard JR, Tang Y, et al. Marked loss of myelinated nerve fibers in the human brain with age. J Comp Neurol. 2003; 462(2):144–152. [PubMed: 12794739]
77. Peters A, Rosene DL. In aging, is it gray or white? J Comp Neurol. 2003; 462(2):139–143. [PubMed: 12794738]
78. Witelson SF, Glezer II, Kigar DL. Women have greater density of neurons in posterior temporal cortex. J Neurosci. 1995; 15(5):3418. [PubMed: 7751921]
79. Schwarb H, Johnson CL, McGarry MDJ, et al. Medial temporal lobe viscoelasticity and relational memory performance. Neuroimage. 2016; 132:534–541. [PubMed: 26931816]
80. Schwarb H, Johnson CL, Daugherty AM, et al. Aerobic fitness, hippocampal viscoelasticity, and relational memory performance. NeuroImage. 2017; 153:179–188. [PubMed: 28366763]
81. Sandroff BM, Johnson CL, Motl RW. Exercise training effects on memory and hippocampal viscoelasticity in multiple sclerosis: a novel application of magnetic resonance elastography. Neuroradiology. 2017; 59(1):61–67. [PubMed: 27889837]
82. Sakai N, Takehara Y, Yamashita S, et al. Shear stiffness of 4 common intracranial tumors measured using MR elastography: comparison with intraoperative consistency grading. Am J Neuroradiol. 2016; 37(10):1851–1859. [PubMed: 27339950]

83. Murphy MC, Huston J 3rd, Glaser KJ, et al. Preoperative assessment of meningioma stiffness using magnetic resonance elastography. J Neurosurg. 2013; 118(3):643–648. [PubMed: 23082888]
84. Hughes JD, Fattahi N, Van Gompel J, et al. Higher-resolution magnetic resonance elastography in meningiomas to determine intratumoral consistency. Neurosurgery. 2015; 77(4):653–658. [PubMed: 26197204]
85. Papazoglou S, Hamhaber U, Braun J, et al. Horizontal shear wave scattering from a nonwelded interface observed by magnetic resonance elastography. Phys Med Biol. 2007; 52(3):675–684. [PubMed: 17228113]
86. Papazoglou S, Xu C, Hamhaber U, et al. Scatter-based magnetic resonance elastography. Phys Med Biol. 2009; 54(7):2229–2241. [PubMed: 19293467]
87. Simon M, Guo J, Papazoglou S, et al. Non-invasive characterization of intracranial tumors by magnetic resonance elastography. New J Phys. 2013; 15(8):085024.
88. Reiss-Zimmermann M, Streitberger KJ, Sack I, et al. High resolution imaging of viscoelastic properties of intracranial tumours by multi-frequency magnetic resonance elastography. Clin Radiol. 2015; 25(4):371–378.
89. Streitberger KJ, Reiss-Zimmermann M, Freimann FB, et al. High-resolution mechanical imaging of glioblastoma by multifrequency magnetic resonance elastography. PLoS One. 2014; 9(10):e110588. [PubMed: 25338072]
90. Pepin KM, McGee KP, Arani A, et al. MR elastography analysis of glioma stiffness and IDH1-mutation status. Am J Neuroradiol. 2018; 39(1):31–36. [PubMed: 29074637]
91. Murphy MC, Jones DT, Jack CR, et al. Regional brain stiffness changes across the Alzheimer's disease spectrum. NeuroImage: Clinical. 2016; 10:283–290. [PubMed: 26900568]
92. Gerischer LM, Fehlner A, Köbe T, et al. Combining viscoelasticity, diffusivity and volume of the hippocampus for the diagnosis of Alzheimer's disease based on magnetic resonance imaging. NeuroImage: Clinical. 2018; 18:485–493. [PubMed: 29527504]
93. Murphy MC, Curran GL, Glaser KJ, et al. Magnetic resonance elastography of the brain in a mouse model of Alzheimer's disease: initial results. Magn Reson Imaging. 2012; 30(4):535–539. [PubMed: 22326238]
94. Munder T, Pfeffer A, Schreyer S, et al. MR elastography detection of early viscoelastic response of the murine hippocampus to amyloid beta accumulation and neuronal cell loss due to Alzheimer's disease. J Magn Reson Imaging. 2018; 47(1):105–114. [PubMed: 28422391]
95. ElSheikh M, Arani A, Perry A, et al. MR elastography demonstrates unique regional brain stiffness patterns in dementias. Am J Roentgenol. 2017; 209(2):403–408. [PubMed: 28570101]
96. Huston J 3rd, Murphy MC, Boeve BF, et al. Magnetic resonance elastography of frontotemporal dementia. J Magn Reson Imaging. 2016; 43(2):474–478. [PubMed: 26130216]
97. Fattahi N, Arani A, Perry A, et al. Magnetic resonance elastography demonstrates increased brain stiffness in normal pressure hydrocephalus. Am J Neuroradiol. 2016; 37(3):462–467. [PubMed: 26542235]
98. Perry A, Graffeo CS, Fattahi N, et al. Clinical correlation of abnormal findings on magnetic resonance elastography in idiopathic normal pressure hydrocephalus. World Neurosurg. 2017; 99:695–700. e691. [PubMed: 28063896]
99. Streitberger K-J, Wiener E, Hoffmann J, et al. In vivo viscoelastic properties of the brain in normal pressure hydrocephalus. NMR Biomed. 2011; 24(4):385–392. [PubMed: 20931563]
100. Lipp A, Skowronek C, Fehlner A, et al. Progressive supranuclear palsy and idiopathic Parkinson's disease are associated with local reduction of in vivo brain viscoelasticity. Eur Radiol. 2018; doi: 10.1007/s00330-017-5269-y
101. Lipp A, Trbojevic R, Paul F, et al. Cerebral magnetic resonance elastography in supranuclear palsy and idiopathic Parkinson's disease. NeuroImage Clinical. 2013; 3:381–387. [PubMed: 24273721]
102. Klein C, Hain EG, Braun J, et al. Enhanced adult neurogenesis increases brain stiffness: in vivo magnetic resonance elastography in a mouse model of dopamine depletion. PLoS One. 2014; 9(3):e92582. [PubMed: 24667730]

103. Hain EG, Klein C, Munder T, et al. Dopaminergic neurodegeneration in the mouse is associated with decrease of viscoelasticity of substantia nigra tissue. PLoS One. 2016; 11(8):e0161179. [PubMed: 27526042]
104. Wuerfel J, Paul F, Beierbach B, et al. MR-elastography reveals degradation of tissue integrity in multiple sclerosis. Neuroimage. 2010; 49(3):2520–2525. [PubMed: 19539039]
105. Fehlner A, Behrens JR, Streitberger KJ, et al. Higher-resolution MR elastography reveals early mechanical signatures of neuroinflammation in patients with clinically isolated syndrome. J Magn Reson Imaging. 2016; 44(1):51–58. [PubMed: 26714969]
106. Streitberger KJ, Fehlner A, Pache F, et al. Multifrequency magnetic resonance elastography of the brain reveals tissue degeneration in neuromyelitis optica spectrum disorder. Eur Radiol. 2017; 27(5):2206–2215. [PubMed: 27572811]
107. Schregel K, Wuerfel E, Garteiser P, et al. Demyelination reduces brain parenchymal stiffness quantified in vivo by magnetic resonance elastography. Proc Natl Acad Sci USA. 2012; 109(17): 6650–6655. [PubMed: 22492966]
108. Weickenmeier J, de Rooij R, Budday S, et al. Brain stiffness increases with myelin content. Acta Biomater. 2016; 42:265–272. [PubMed: 27475531]
109. Riek K, Millward JM, Hamann I, et al. Magnetic resonance elastography reveals altered brain viscoelasticity in experimental autoimmune encephalomyelitis. NeuroImage: Clinical. 2012; 1(1):81–90. [PubMed: 24179740]
110. Millward JM, Guo J, Berndt D, et al. Tissue structure and inflammatory processes shape viscoelastic properties of the mouse brain. NMR Biomed. 2015; 28(7):831–839. [PubMed: 25963743]
111. Romano A, Guo J, Prokscha T, et al. In vivo waveguide elastography: Effects of neurodegeneration in patients with amyotrophic lateral sclerosis. Magn Reson Med. 2014; 72(6): 1755–1761. [PubMed: 24347290]
112. Waller A. Experiments on the section of the glossopharyngeal and hypoglossal nerves of the frog, and observations of the alterations produced thereby in the structure of their primitive fibres. Philos Trans R Soc Lond B Biol Sci. 1850; 140:423–429.
113. Coleman MP, Conforti L, Buckmaster EA, et al. An 85-kb tandem triplication in the slow Wallerian degeneration (Wld(s)) mouse. Proc Natl Acad Sci USA. 1998; 95(17):9985–9990. [PubMed: 9707587]
114. Romano A, Szymczak W, Okamoto R, et al. Moderate to severe TBI studies using mixed model inversions. Proceedings of the First International MRE Workshop, Berlin Germany. Sep 28–29.2017 :34.
115. Boulet T, Kelso ML, Othman SF. Microscopic magnetic resonance elastography of traumatic brain injury model. J Neurosci Methods. 2011; 201(2):296–306. [PubMed: 21871490]
116. Boulet T, Kelso ML, Othman SF. Long-term in vivo imaging of viscoelastic properties of the mouse brain after controlled cortical impact. J Neurotrauma. 2013; 30(17):1512–1520. [PubMed: 23534701]
117. Feng Y, Gao Y, Wang T, et al. A longitudinal study of the mechanical properties of injured brain tissue in a mouse model. J Mech Behav Biomed Mater. 2017; 71:407–415. [PubMed: 28412646]
118. Badachhape AA, Okamoto RJ, Johnson CL, et al. Relationships between scalp, brain, and skull motion estimated using magnetic resonance elastography. J Biomech. 2018; doi: 10.1016/j.jbiomech.2018.03.028
119. Barnhill E, Hollis L, Sack I, et al. Nonlinear multiscale regularisation in MR elastography: Towards fine feature mapping. Med Image Anal. 2017; 35:133–145. [PubMed: 27376240]
120. Fehlner A, Hirsch S, Weygandt M, et al. Increasing the spatial resolution and sensitivity of magnetic resonance elastography by correcting for subject motion and susceptibility-induced image distortions. J Magn Reson Imaging. 2017; 46(1):134–141. [PubMed: 27764537]
121. Hetzer S, Birr P, Fehlner A, et al. Perfusion alters stiffness of deep gray matter. J Cereb Blood Flow Metab. 2018; 38(1):116–125. [PubMed: 28151092]

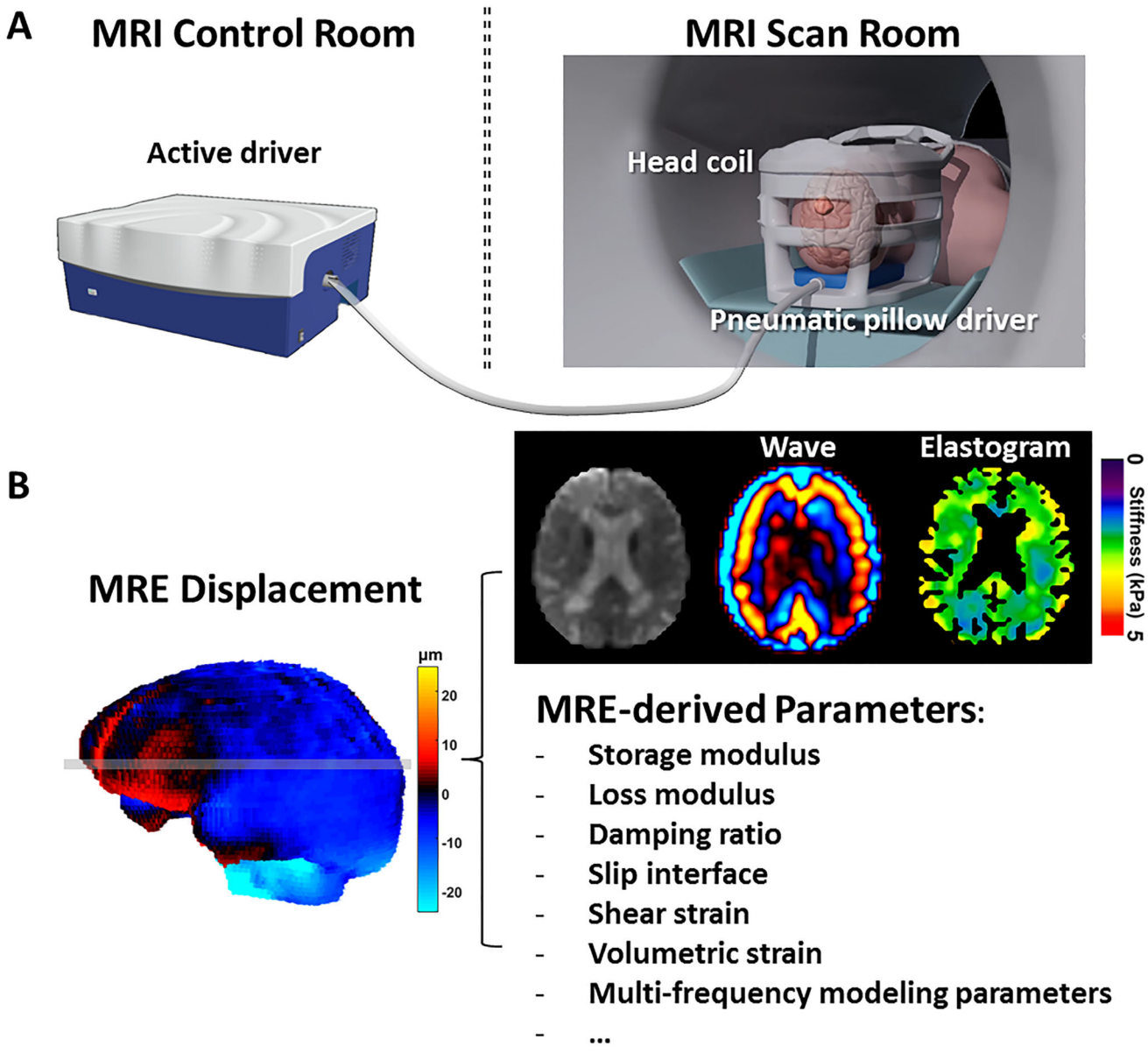

Figure 1.

(**A**) Schematic diagram of brain MRE setup with a pneumatic pillow driver. (**B**) Illustration of MRE wave image and stiffness map (elastogram) as well as a brief list of mechanical parameters that can be extracted from brain MRE.

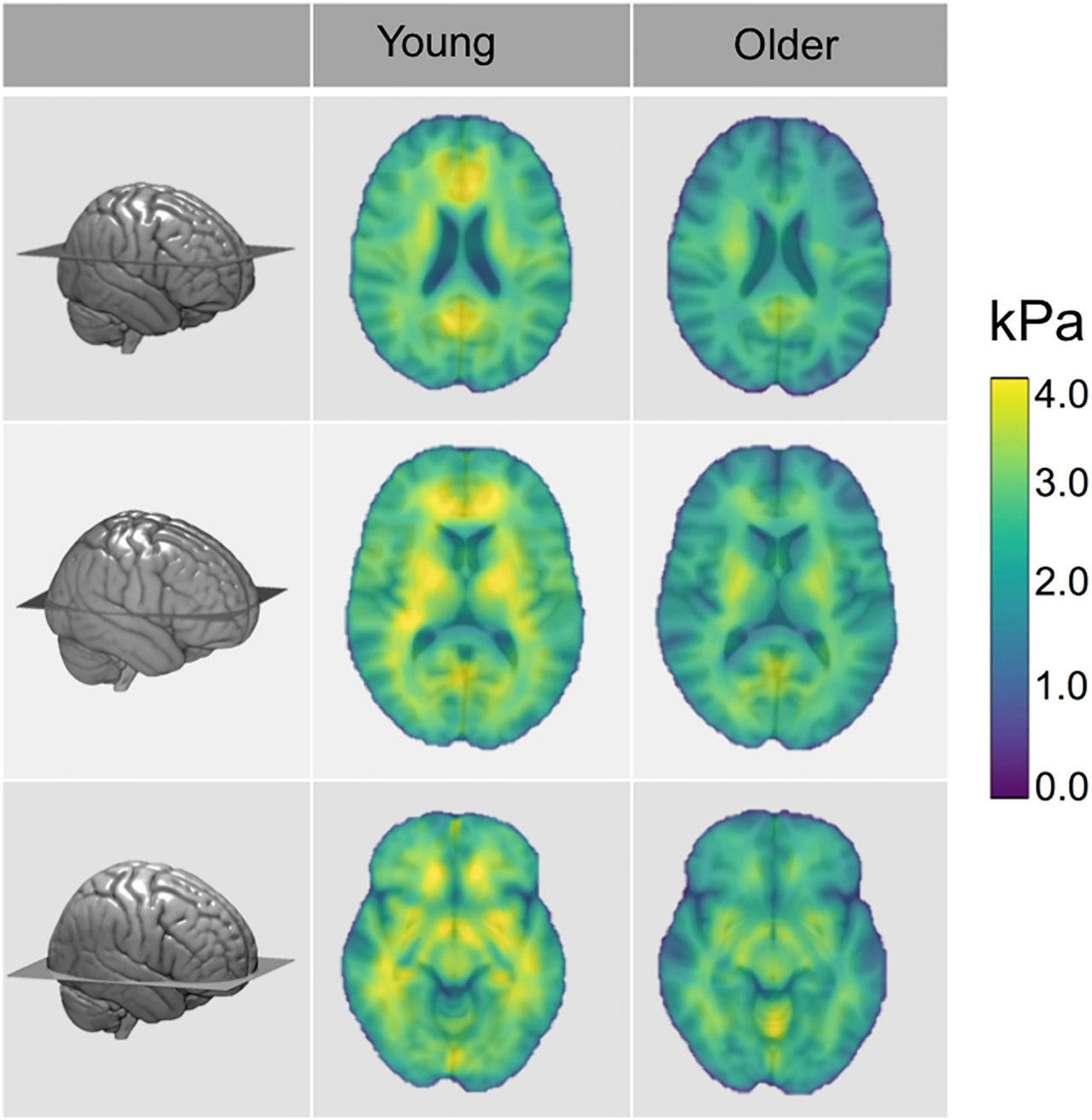

Figure 2.

High resolution mean MRE stiffness maps of young and older adults transformed into standard Montreal Neurological Institute (MNI) space, demonstrating widespread softer brains with aging ($p < 0.001$). (From *Hiscox LV, et al. High-resolution magnetic resonance elastography reveals differences in subcortical gray matter viscoelasticity between young and healthy older adults. Neurobiol Aging 2018;65:158–167*. Reproduced with permission from Elsevier).

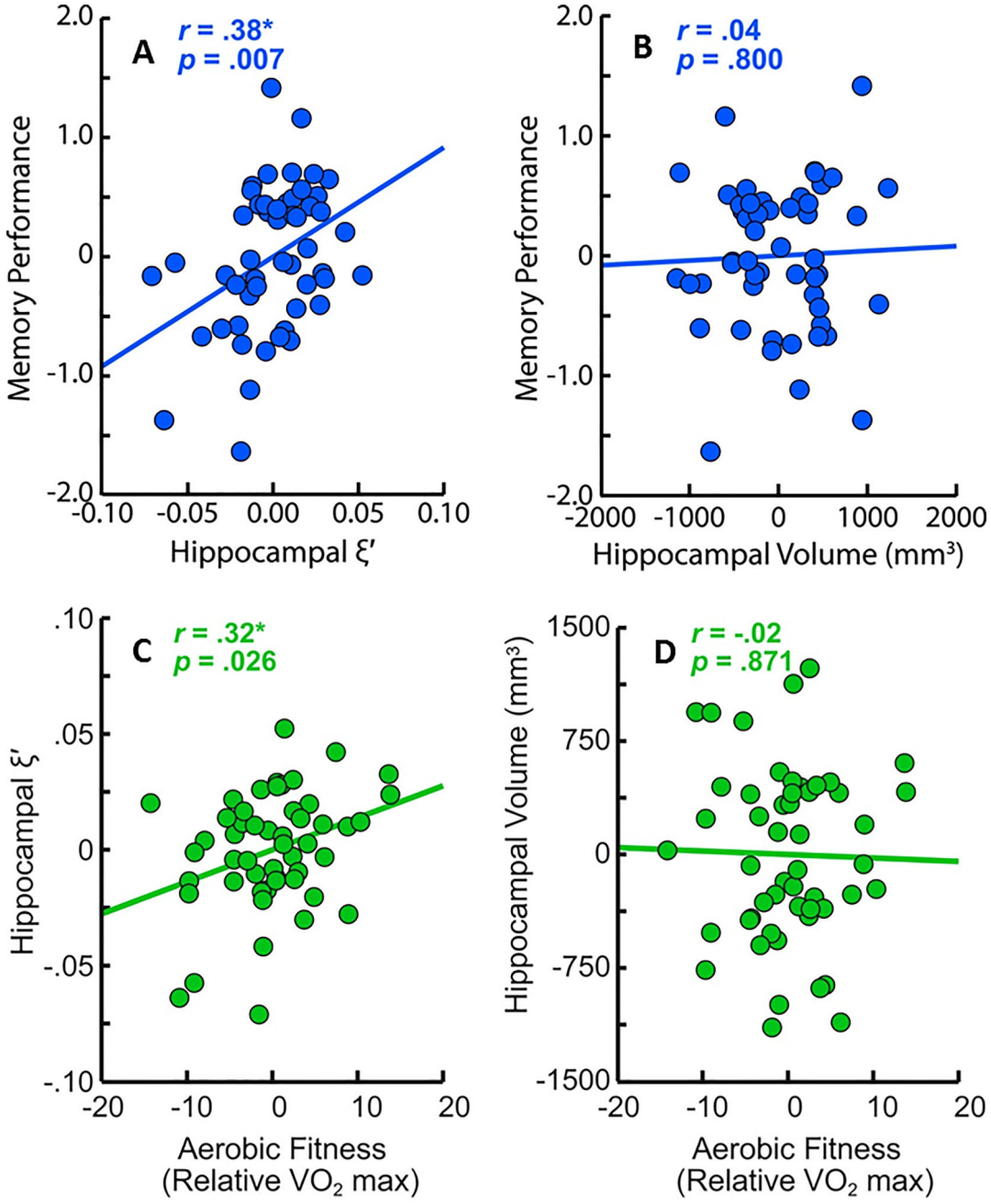

Figure 3.

Correlations between both hippocampal damping ratio and volume with memory performance and aerobic fitness. The significant positive correlations for damping ratio indicate the more the hippocampus behaves like an elastic solid, the better an individual's memory performance and the more fit an individual is. No correlation is found between hippocampal volume and task performance as well as aerobic fitness. The quantity depicted as hippocampal ξ' is the difference from the group mean of the adjusted damping ratio 1-ξ. (From *Schwarb H, et al. Aerobic fitness, hippocampal viscoelasticity, and relational memory performance. NeuroImage 2017;153:179–188.* Reproduced with permission from Elsevier).

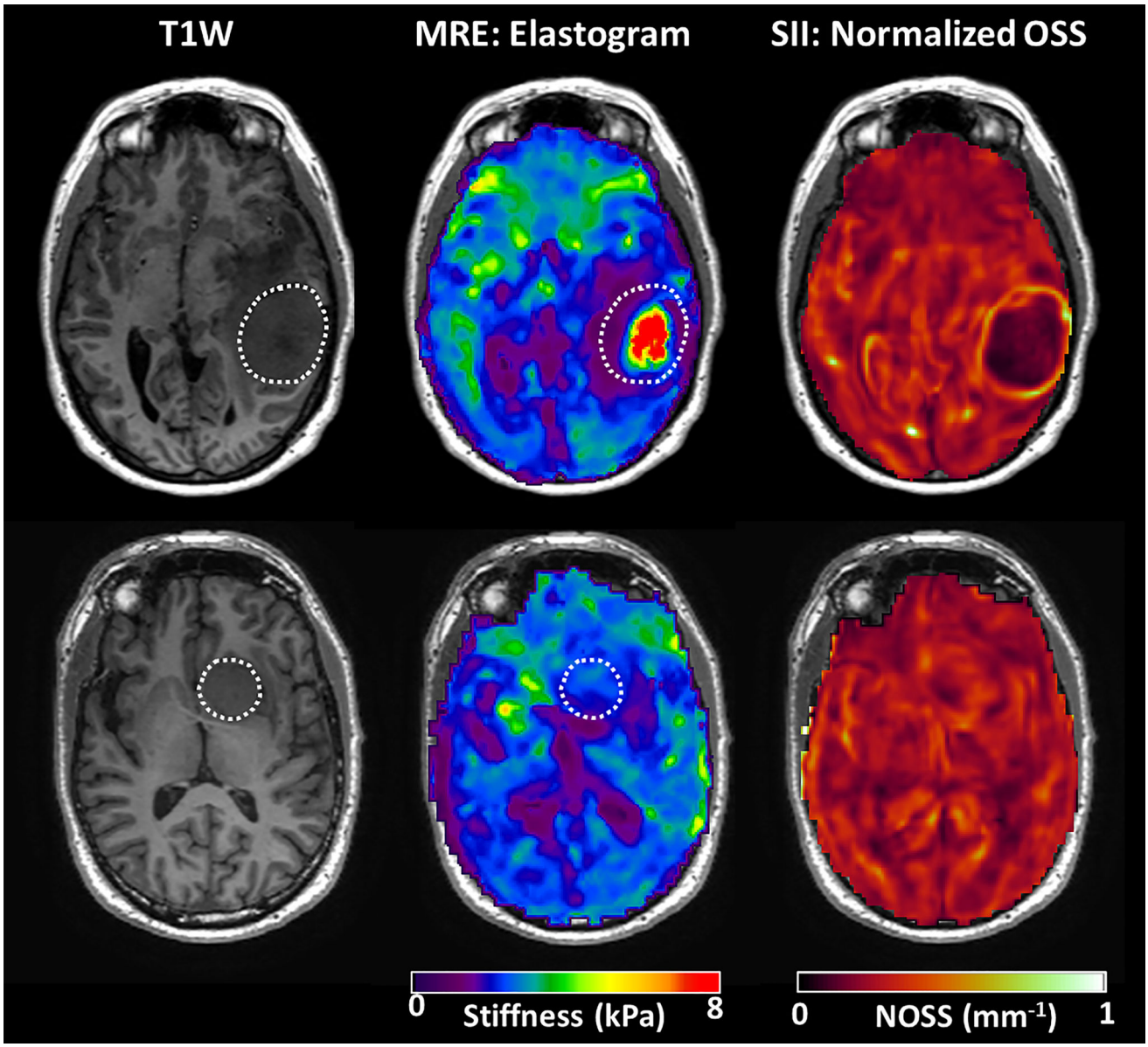

Figure 4.

Example MRE and SII images from a firm/non-adherent meningioma (top) and an intermediate soft/adherent meningioma (bottom). The stiffness maps are shown in the middle column and SII measured normalized octahedral shear strain (NOSS) maps are shown in the right column. The tumor-brain slip interface is clearly defined with the NOSS map in the top row, indicating no adhesion, which is absent in the adherent case in the bottom. Both cases are consistent between MRE/SII assessment and surgical findings of tumor consistency and adherence.

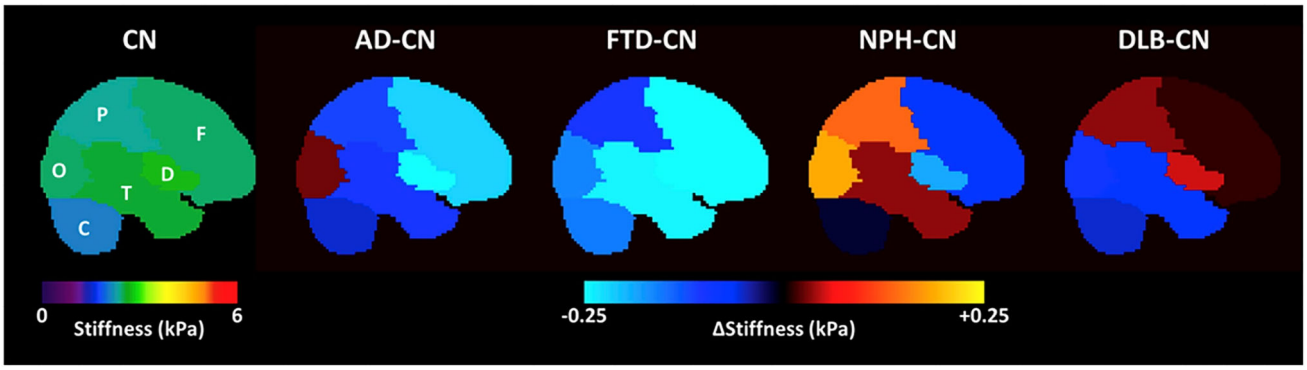

Figure 5.

Summary diagram of regional stiffness changes in patients with Alzheimer's disease (AD), frontotemporal dementia (FTD), normal pressure hydrocephalus (NPH), and dementia with Lewy bodies (DLB) compared with cognitively normal control (CN) subjects. The left panel is a sagittal view of a lobar brain atlas color-coded with each region's mean stiffness in CN group. The right four panels show the mean stiffness difference between the dementia groups and the CN group in each region. F: frontal lobe; P: partial lobe; T: temporal lobe; O: occipital lobe; D: deep gray and white matter; C: cerebellum. (From *Murphy MC, et al. MR elastography of the brain and its application in neurological diseases. NeuroImage 2017*. Reproduced with permission from Elsevier).

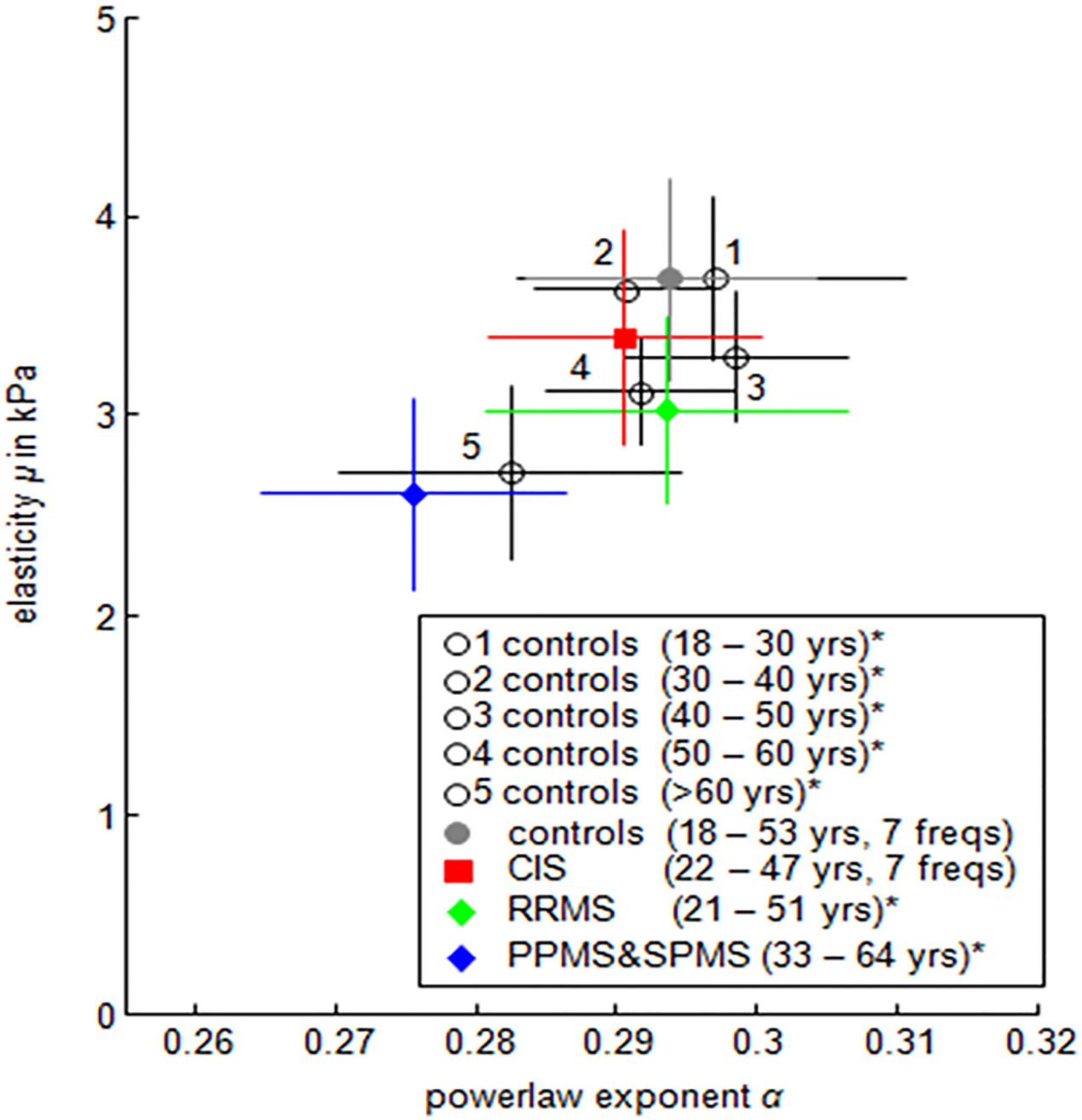

Figure 6.

Group mean viscoelastic parameters of MRE in three stages of multiple sclerosis (MS): clinically isolated syndrome (CIS), relapsing-remitting multiple sclerosis (RRMS), and primary or secondary chronic-progressive MS (PPMS&SPMS). The two parameters (shears elasticity μ and powerlaw exponent α) are calculated from a springpot model fitted to storage and loss moduli at multiple frequencies. (From *Fehlner A, et al. Higher-resolution MR elastography reveals early mechanical signatures of neuroinflammation in patients with clinically isolated syndrome. J Magn Reson Imaging 2016;44(1):51–58*. Reproduced with permission from John Wiley and Sons).

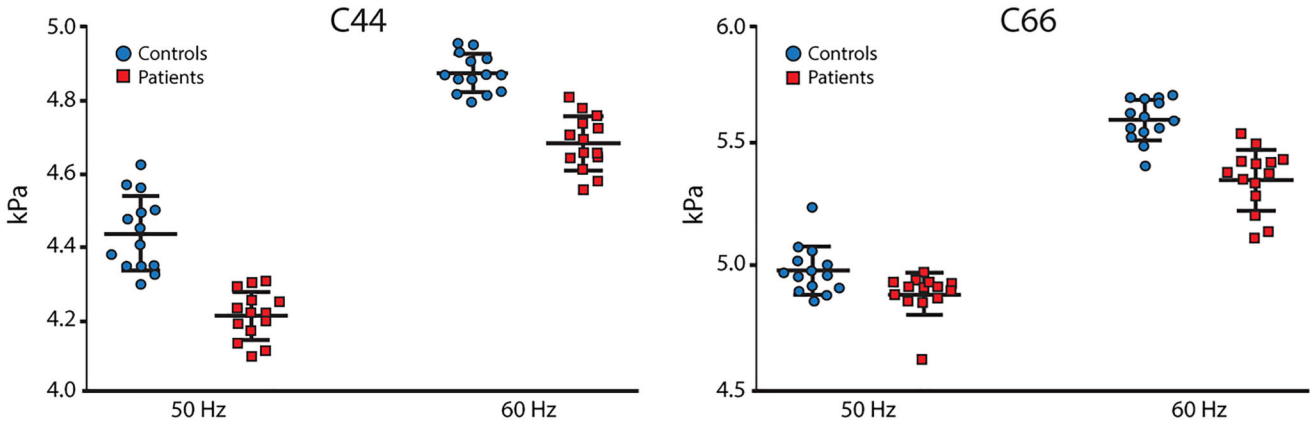

Figure 7.

Mean values and standard deviations of the real components of anisotropic shear stiffness evaluated along the corticospinal tracts (CSTs) with right and left structures combined for each control (blue dots) and ALS patients (red squares) at 50 and 60 Hz temporal excitation frequencies. C44 (left image) is the shear stiffness polarized parallel to the principal CST fiber direction, while C66 (right image) is the shear stiffness polarized perpendicular to the principal CST fiber direction. Both C44 and C66 are significantly lower in ALS patients compared to the healthy controls. (From *Romano A, et al. In Vivo Waveguide Elastography: Effects of Neurodegeneration in Patients with Amyotrophic Lateral Sclerosis. Magn Reson Med 2014;72:1755–1761.* Reproduced with permission from John Wiley and Sons).

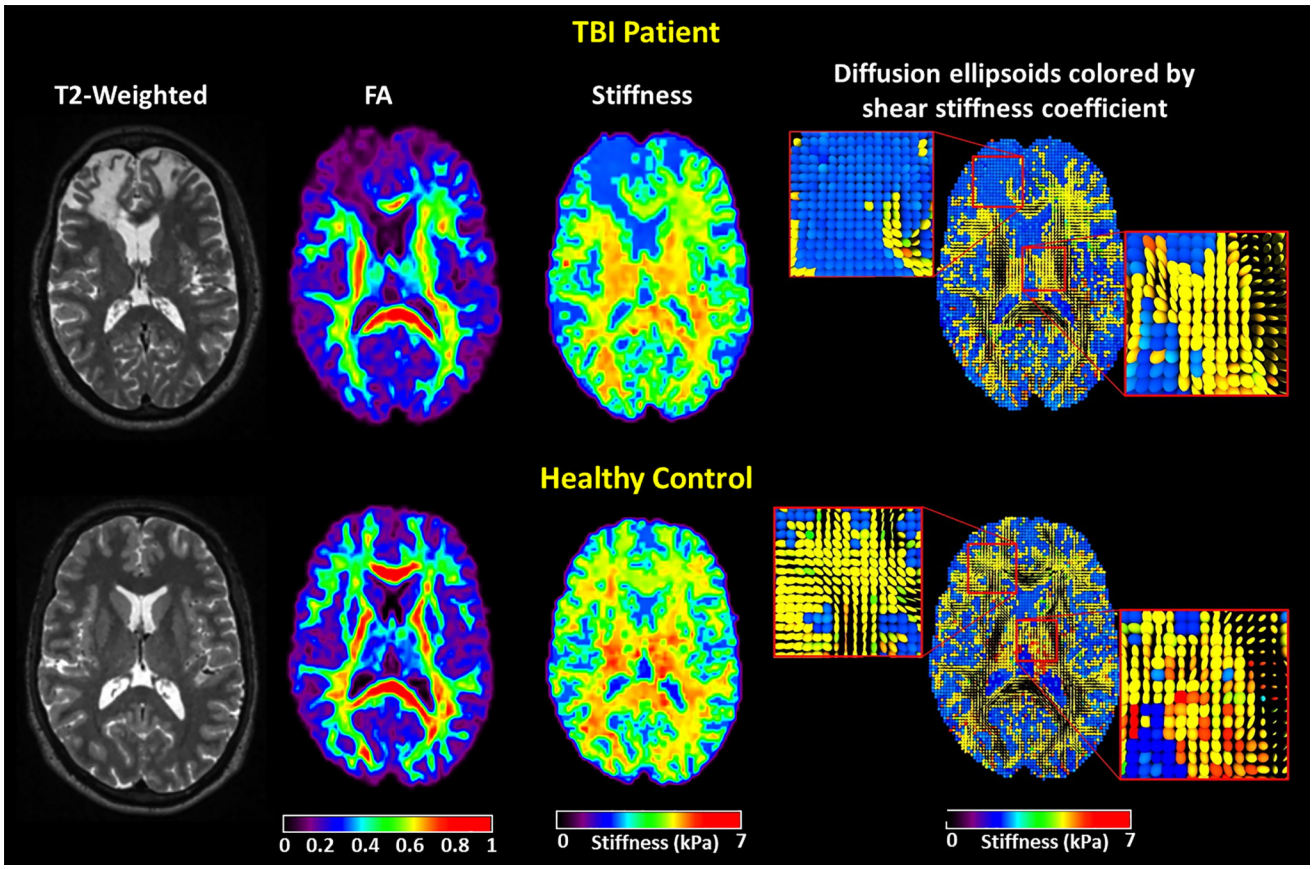

Figure 8.

Comparison of MMI results between a severe TBI patient (top panel) and a healthy control (bottom). The first column is the transverse anatomical T2-weighted images showing a lesion in the right frontal lobe of the patient. The second column is FA maps showing the magnitude range from 0–1. The third column is the MMI estimates of isotropic shear stiffness in gray matter and the lesion, and anisotropic shear stiffness coefficient, C_{44}, in white matter. The last column shows diffusion ellipsoids colored by isotropic and anisotropic shear stiffness, C_{44} in white matter. The right portion of the normally anisotropic forceps minor in the patient has been damaged and replaced with a soft, isotropic lesion. (From *Romano A, et al. Moderate to severe TBI studies using mixed model inversions. Proceedings of the First International MRE Workshop, Berlin Germany, September 28–29, 2017, pp 34.*)